Journal of Structural Chemistry. Vol. 57, No. 7, pp. 1369-1376, 2016.

MODELLING OF SUBSTITUTIONAL DEFECTS IN THE STRUCTURE OF Ti-BEARING HIBONITE

I. A. Pankin, A. N. Kravtsova*, O. E. Polozhentsev, and A. V. Soldatov

UDC 539

A local atomic structure around titanium positions in Ti-bearing hibonite ($CaAl_{12}O_{19}$) has been studied. The structural models of substitution of different substitution defects Ti–Al in hibonite by titanium atoms have been considered. Optimization of structural models of hibonite has been done by means of density functional theory calculations using pseudopotential approximation as implemented in VASP 5.3 code. Gibbs free energies analysis has shown that models of substitution of M2 and M4 aluminum positions by titanium atoms are the most probable. For the most probable structural models of Ti-bearing hibonite theoretical X-ray absorption near-edge structure (XANES) spectra near the titanium *K* edge have been calculated. Significant differences in theoretical XANES spectra calculated for different structural models with non-optimized and optimized atomic structure have been demonstrated. Changes in the intensity of pre-edge structure of Ti*K* XANES spectra for different substitution models of aluminum by titanium have been observed which relate to different titanium coordination in structural models. Energy shift of spectral features towards lower energy for optimized models implies increase of interatomic distances in local surroundings of Ti absorbing atoms.

DOI: 10.1134/S0022476616070106

Keywords: local atomic structure, geological materials, hibonite, computer modeling, density functional theory, XANES spectroscopy.

INTRODUCTION

Calcium-aluminum inclusions of hondrite meteorites are among the oldest materials in Solar System [1]. Hibonite ($CaAl_{12}O_{19}$) is a mineral found in these inclusions. It can incorporate in its structure significant amount of polyvalent elements such as V, Cr, Fe and Ti. It was discussed that hibonite is potentially useful for determination of conditions that occurred in the early Solar System, in particular, oxygen fugacity (f_{O_2}). For terrestrial samples the ratio Fe^{2+}/Fe^{3+} can be used to estimate oxygen fugacity which is not appropriate for calcium-aluminum inclusions of hondrite materials as conditions of their formation leads to the formation of metallic iron. In this case the possibility of alternative estimation of f_{O_2} on the basis of Ti^{3+}/Ti^{4+} analysis was discussed [2].

Hibonite ($CaAl_{12}O_{19}$) has complex hexagonal structure formed by layers of polyhedra that are perpendicular to *c* axis. In the hibonite structure calcium is 12-coordinated and aluminum is distributed over five (M) positions. The structure of hibonite was sequentially refined in [3-8]. The structure of Ti-bearing hibonite was discussed in [6, 8, 9-11].

International Research Center "Smart Materials", Southern Federal University, Rostov-on-Don, Russia; *akravtsova@sfedu.ru. Translated from *Zhurnal Strukturnoi Khimii*, Vol. 57, No. 7, pp. 1445-1452, September-October, 2016. Original article submitted December 12, 2015.

The goal of the present investigation is to study local atomic structure around titanium positions in hibonite on the basis of computer modeling using density functional theory in conjunction with pseudopotentials as implemented in VASP 5.3 code. In the paper the defects of substitution of different aluminum positions by titanium atoms are considered; the probabilities of defects are estimated; the Ti–O bond lengths of most stable structures are analyzed. For verification of results of computer modeling it is desirable to attract experimental methods. The modern effective method allowing selective determination of local atomic structure around certain type of atoms in materials without long-range order in atomic distribution is X-ray Absorption Near-Edge Structure (XANES) spectroscopy [12]. To verify parameters of local atomic structure of Ti-bearing hibonite and to study its charge state experimental Ti *K* edge XANES spectra are needed. In the present work for most stable structures of Ti-bearing hibonite obtained by computer modelling the theoretical XANES spectra have been calculated and analyzed.

METHODS OF CALCULATIONS

Optimization of atomic structure of pure hibonite and Ti-bearing hibonite has been performed using VASP 5.3 code (Vienna *Ab-Initio* Simulation Package) [13]. Methods of calculations realized in VASP 5.3 code are based on density functional theory using periodic boundary condition and pseudopotential approximation which significantly reduce the computational cost of the problem.

PAW-PBE (projector augmented-wave Perdew-Burke-Ernzerhof) type pseudopotentials [14] were used and atomic positions were optimized by means of energy minimization using conjugate gradients method [15]. Self-consistent field (SCF) cycles of electron density were calculated using Davidson scheme [16]. The energy convergence condition was set up as $0.5 \cdot 10^{-3}$ eV. A kinetic energy cutoff of 450 eV was used for the plane wave basis set. For sampling of the Brillouin zone a Monkhrost–Pack algorithm was used. A 11×11×5 *k*-point mesh was automatically generated for the unit cell of hibonite since it has a hexagonal lattice and the module of **c** vector significantly exceeds the module of **a** and **b** vectors.

As initial structures of hibonite ($CaAl_{12}O_{19}$) preceding the titanium doping and geometry optimization procedure two structures determined in [4] and [6] were used. Hibonite has hexagonal structures (*P*63/*mmc* space group) with $a = 5.564$ Å, $c = 21.892$ Å lattice parameters according to [4] and $a = 5.613$ Å, $c = 22.285$ Å according to [6]. The structure of hibonite is formed by polyhedral layers perpendicular to *c* axis, in which calcium is 12-coordinated and aluminum is distributed over five (M) positions. Literature sources [4] and [6] use different numeration of aluminum (M) atomic positions. Multiplicity and coordination of atomic positions of hibonite structure from K. Kato et al. [4] can be described as $^{[12]}Ca^{[6]}M1_6{}^{[4]}M2_2{}^{[6]}M3_2{}^{[6]}M4^{[5]}M5O_{19}$, where multiplicity of atomic positions is shown by lower indexes and coordination numbers are presented by upper indexes in square brackets. For more resent works including V. V. Bermanec et al. [6] the multiplicity of atomic positions and coordination numbers can be described as $^{[12]}Ca^{[6]}M1^{[5]}M2^{[4]}M3_2{}^{[6]}M4_2{}^{[6]}M5_6O_{19}$. Further a newer numeration of metallic atomic positions of hibonite from [6] will be used, and equivalence between positions from [4] and [6] will be done where it is necessary. Also, the difference between two considered structures is that M2 atomic position in work [6] is split into two symmetrically equivalent positions with half-occupation obtained by the displacement of M2 cation from central position above and below the equatorial plane of bipyramid. The impurities of low concentration in $CaAl_{12}O_{19}$ mineral were not taken into account when calculations using structure from [6] were done.

Single-atom and multi-atom substitutional Ti–Al defects for different aluminum positions were considered.

Ti *K* edge XANES spectra for most probable defects of substitution of aluminum positions by titanium which were obtained as results of comparison of Gibbs free energies for optimized structural models were calculated using both full multiple scattering method within Green's function formalism and *muffin-tin* approximation for the shape of crystal potential (FEFF 9.6.4 code [17, 18]) and full-potential finite difference method [3] (FDMNES program code [19]). Updated version of FDMNES software can significantly reduce the computation cost of calculations in full potential of absorption spectra by using Sparce Solvers in the process of finite differences matrix diagonalization [20]. XANES spectra were calculated using the Hedin-Lundquist type of exchange-correlation potential taking into account the core hole created by electron transition.

Structure modeling and calculation of absorption spectra were done using supercomputer “Blokhin” of IRC “Smart materials” of Southern Federal University.

RESULTS AND DISCUSSION

With the aim to investigate the structure of Ti-bearing hibonite, modelling of a number of single-atom and multi-atom defects of substitution of different nonequivalent aluminum positions in hibonite structure ($CaAl_{12}O_{19}$) by titanium atoms. As initial structural models of hibonite (without titanium impurities) the structures obtained by K. Kato et al. [4] and V. V. Bermanec et al. [6] (see section “Methods of calculations”).

On the first stage the multi-atom defects of substitution of different aluminum positions by titanium in initial structures from [4] and [6] (i.e., titanium atoms replace all aluminum atoms in considered crystallographic non-equivalent position) were studied. Optimization of structures with titanium defects were not carried out. Table 1 shows the values of Gibbs free energies calculated using VASP 5.3 code for each structural model of multi-atom substitution of aluminum positions in hibonite (structure from [6]). It was found that in the case of modelling of multi-atom substitution defects, the defects of substitution of aluminum positions located in M5 by titanium atoms (atomic positions numeration from [6]) are most probable. It should be noted that in the case of multi-atom substitution defect, there are twelve titanium atoms per hibonite unite cell at Ti→M5 type substitution. Thus, Ti–Ti interactions may provide a significant contribution to the total energy of the system.

Further, single-atom substitution defects (titanium atom replace only one aluminum atom in a certain crystallographic position in unit cell of hibonite) were considered. In investigated objects titanium concentration is not high, so, single-atom substitution defects are physically grounded. Table 2 shows calculated values of Gibbs free energies for hibonite structure (from [6]), in which titanium atom substitutes aluminum atoms located in different crystallographic positions. On this stage the optimization of hibonite structure after substitution of aluminum atoms by titanium were not taken into account. Table 2 also summarizes changes in the Gibbs free energy (differences between the value of Gibbs free energy for cell without substitution of aluminum atoms by titanium and the one with substitution) per one atom. According to the results of modelling of Ti→Al single-atom substitution defect, it was established that defects of substitution by Ti of Al atoms located in non-equivalent positions M2 and M4 (numbering of atomic position according to V. V. Bermanec et al. [6]) are the most probable. The change in Gibbs free energy per one titanium atom is less in the case of single-atom defects then the one in the case of multi-atom defects that can be explained by significant contribution of Ti–Ti interactions to minimization of full energy of the system which occur during the simulation of multi-atom substitution defects. Single-atom substitutions of aluminum positions by titanium in the structure of K. Kato et al. [4] has shown that the most probable defects

TABLE 1. Gibbs Free Energy for Multi-Atom Substitutional Defects for Different Non-Equivalent Al Positions in the Hibonite Structure Reported by V. Bermanec et al. [6]

Type of substitution	Number of Ti→Al substitutions per unit cell	Gibbs free energy, eV	Changes of Gibbs free energy per Ti atoms, eV
Without substitution	0	–475.1838	–
Ti → M1 (M4)	2	–476.3118	0.5637
Ti → M2 (M5)	2	–479.0056	2.1250
Ti → M3 (M2)	4	–481.5628	1.5948
Ti → M4 (M3)	4	–484.1805	2.2492
Ti → M5 (M1)	12	**–501.1238**	2.0783

Numeration of atomic Al sites in accordance with [6] is in first column, numeration of Al sites in accordance with [4] is represented in parenthesis. Total energy differences of the cell without titanium substitution for aluminum sites and the cells with substitutions are also presented (fourth column).

TABLE 2. Gibbs Free Energy for Single-Atom Substitutional Defects for Different Non-Equivalent Al Positions in the Hibonite Structure from [6] (without successive structural optimization).

Type of substitution	Number of Ti→Al substitutions per unit cell	Gibbs free energy, eV	Changes of Gibbs free energy per Ti atom, eV
Without substitution	0	–475.1838	-
Ti → M1 (M4)	1	–475.8631	0.6793
Ti → M2 (M5)	1	**–477.0589**	**1.8752**
Ti → M3 (M2)	1	–476.7467	1.5630
Ti → M4 (M3)	1	**–477.3215**	**2.1377**
Ti → M5 (M1)	1	–476.5607	1.3769

Numeration of atomic Al sites in accordance with [6] is in the first column, numeration of Al sites in accordance with [4] is represented in brackets. The differences in the free energy between defect models and pure hibonite structure are in fourth column.

are those of substitution by titanium of Al atoms in positions M3 and M5 that correspond to M2 and M4 positions in numeration of V. V. Bermanec et al. Further in the text we will use the numeration of atomic positions from the paper of V. V. Bermanec et al.

On the next stage of investigation the optimization of the structure of hibonite ($CaAl_{12}O_{19}$) determined in [6] was done. According to the results of optimization there were no significant changes in unit cell volume, unit cell shape and atomic position as compared with the values described in [6]. Further the obtained optimized structure of hibonite was used to model single-atom defects of substitution by titanium. Then, structure models with substitution of different aluminum positions by titanium were optimized using VASP 5.3 code that allowed to obtain more energetically favorable and stable structural models for defects of aluminum substitution by titanium as compared with models without geometry optimization. Table 3 presents the results of modelling of single-atom substitution defect with preliminary geometry optimization for initial structure of hibonite and following optimization of hibonite structure with titanium defects. For clarity, Fig. 1 shows a histogram of obtained values of Gibbs free energies for different single-atom defects of substitution of aluminum positions by titanium. From Table 3 and Fig. 1 it can be seen that, as before, defects of substitution of aluminum positions M2 and M4

TABLE 3. The Results of Modelling the Ti–Al Single-Atom Substitutional Defect with Regard to the Structural Pre-Optimization of the Pure Hibonite Structure from [6] and Successive Geometry Optimization for the Defect Models

Type of substitution	*a*/*c*	$V_{\text{unit cell}}$	Gibbs free energy, eV	Changes of Gibbs free energy per Ti atoms, eV
Without substitutions (structure as described in [6])	0.2519	608.04	–475,1838	
Without substitutions (after optimizations)	0.2537	600.24	–475.5174	0.3336
Ti → M1	0.2536	606.22	–477.2446	2.0608
Ti → M2	0.2554	605.60	**–477.7217**	**2.5379**
Ti → M3	0.2537	606.43	–477.5788	2.3946
Ti → M4	0.2519	609.11	**–477.9515**	**2.7677**
Ti → M5	0.2537	605.39	–477.5784	2.3947

The ratio of lattice parameters *a*/*c* (first column), cell volume (second column), Gibbs free energy (third column), and differences of Gibbs free energy per Ti atom calculated for optimized defect models and initial pure hibonite structure (fourth column).

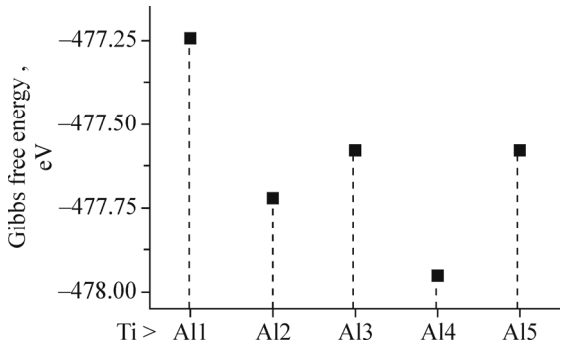

Fig. 1. Gibbs free energy for different single-atom Ti–Al substitutional defects calculated taking into account structural pre-optimization for the pure hibonite [6] and successive optimization for defect models.

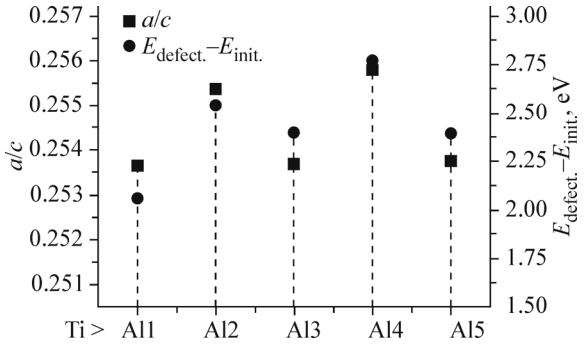

Fig. 2. The ratio of the unit cell lattice parameters (a/c) and differences in the Gibbs free energy between the Ti→Al substitutional defect models and pure hibonite structure ($E_{defect} - E_{init}$) calculated for different non-equivalent positions of Al atoms.

by titanium are most probable. For models of substitution by titanium of M2 and M4 positions the differences in energy relative to the structures without defects are 2.537 eV and 2.768 eV, respectively, as compared to 1.875 eV and 2.138 eV for substitution models without geometry optimization (Table 2). In Fig. 2 for different models of substitution of aluminum by titanium the ratio of translation vectors of hexagonal cell a/c, as well as the difference in Gibbs free energy per one titanium atom for structure with defect and without defect are presented. It can be seen that energetically more favorable models (replacement of M2 and M4 positions by titanium) undergo larger deformations of unit cell (larger values of the ratio of translation vectors a/c). Table 4 shows the obtained cell parameters a and c of hibonite, ratio a/c and volume of unit cell obtained as results of geometry optimization with single-atom defects of substitution of different aluminum positions by titanium.

In Table 5 for most probable models of substitution of M2 and M4 by titanium we present the interatomic distances between titanium atoms and closest oxygen atoms for initial (nonoptimized) and optimized structures. The increase in Ti–O interatomic distance is observed as a result of optimization which is due to the higher values of ionic radius of Ti atoms in comparison with Al.

To verify the structure parameters resulting from the atomic geometry optimization it is desirable to attract experimental methods of analysis of materials structure. Modern technique allowing to analyze 3D atomic structure around certain type of atoms in materials including those without long-range order in atomic distribution is X-ray Absorption Near-Edge Structure (XANES) spectroscopy. Recently, XANES spectroscopy has been successfully applied to study objects without long-range structure [21, 22] and geological materials [23, 24]. However, it should be noted that the method of extraction of structural information from experimental X-ray absorption near-edge structure spectra is not direct and demands theoretical modelling of XANES spectra. In the work for energetically most stable structures of hibonite with substitution of aluminum positions by titanium (five-coordinated titanium in M2 substitution position and six-coordinated titanium in M4 substitution position), which were obtained as a result of computer modelling using VASP 5.3 code, the theoretical TiK edge

TABLE 4. Lattice Parameters of the Unit Cell a and c, Ratio of Lattice Parameters a/c, Cell Volume Obtained for Optimized Ti–Al Single-Atom Substitutional Defect Models for Different Non-Equivalent Positions of Al Atoms

Type of substitution	a	c	a/c	Cell volume
Ti → M1	5.622	22.144	0.2539	606.30
Ti → M2	5.631	22.068	0.2552	606.12
Ti → M3	5.619	22.189	0.2533	606.89
Ti → M4	5.636	22.099	0.2551	609.61
Ti → M5	5.622	22.143	0.2538	605.57

TABLE 5. The Ti–O Interatomic Distances in the Nearest Surroundings of Ti Atoms for Initial (non-optimized) and Final (optimized) Structural Models for Ti–Al Single-Atom Substitutions*

Type of substitution	Nearest neighbors	Ti–O distances before structural optimization, Å	Ti–O distances after structural optimization, Å	Changes of Ti–O interatomic distances in result of geometry optimization, Å
Ti → M2	O	1.7802	1.8602	0.0800
	O	1.7802	1.8602	0.0800
	O	1.7802	1.8603	0.0801
	O	2.0012	2.2451	0.2439
	O	2.5405	2.2621	–0.2784
Ti → M4	O	1.8829	1.9998	0.1169
	O	1.8829	1.9998	0.1169
	O	1.8829	2.0000	0.1171
	O	2.0118	2.0817	0.0699
	O	2.0118	2.0819	0.0701
	O	2.0118	2.0820	0.0702

* The Ti–O interatomic distances are presented for the most probable defect structural models (Ti on M2 and M4 positions).

XANES were calculated. XANES spectra were calculated as for initial structural models prior the structure optimization as for structural models with following optimization of atomic structure. Obtained spectra are presented in Fig. 3.

According to the results of simulation of Ti *K* edge spectra it can be seen that XANES spectroscopy is a technique which is sensitive to changes in local atomic arrangement of titanium atoms in hibonite resulting from geometry optimization. Changes in the spectral shape and energy positions of main features are observed both in the calculations of full multiple scattering (Fig. 3*a*) and full-potential finite difference method (Fig. 3*b*). There is a redistribution of intensities (increase in the intensity of the main peak – "white line") near the absorption edge region for structural models of substitution defect of Ti on M2 position before and after geometry optimization. For both most probable substitution defects – Ti atoms on M2 and M4 aluminum positions – there is tendency to reduce the energy separation between spectral maxima if comparing spectra calculated for structural models before and after geometry optimization, which is in the good agreement with the increase of Ti–O distances according to semi-empirical Natoli's rule [25]. The increase of the pre-edge feature intensity of the Ti *K* edge XANES spectra is observed when titanium coordination decreases. Analysis of the experimental Ti *K* edge spectra of

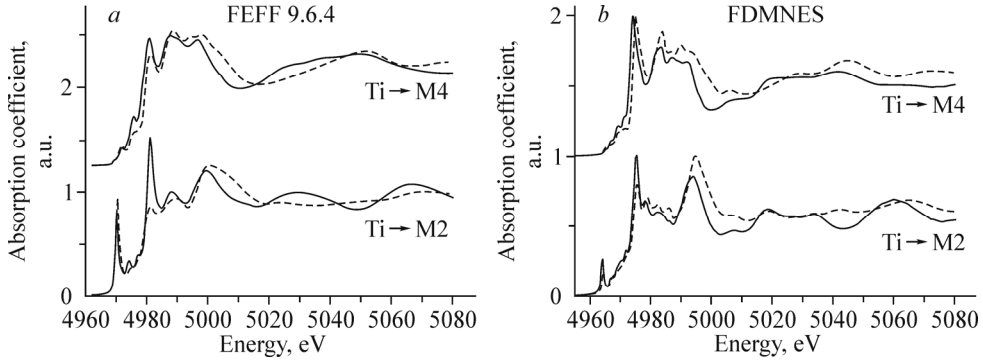

Fig. 3. Theoretical Ti *K* edge XANES spectra of hibonite simulated for the substitutional models of Ti on M2 and M4 positions. The spectra calculated for the models before and after structural optimization are shown in dotted and solid lines, respectively. The simulations were performed using full multiple scattering approach as implemented in FEFF9.6.4 code (*a*) and full potential finite difference method as implemented in FDMNES code (*b*).

Ti-bearing hibonite in comparison with those for comparison pattern will allow making more detailed conclusions on local atomic structure as well as on oxygen stage of titanium atoms in investigated objects. Moreover, because of significant difference in the shape of absorption spectra for two more probable defects of substitution of M2 and M4 positions by Ti, comparison of these theoretical spectra with an experimental one will allow to estimate probabilities of location of Ti atoms on M2 and M4 positions in investigated samples.

CONCLUSIONS

The structure of hibonite ($CaA_{l2}O_{19}$) and Ti-bearing hibonite was studied by DFT-based calculations using pseudopotential approximation as implemented in VASP 5.3. Gibbs free energies were obtained for the different single-atom Ti–Al replacement defects in the structure of hibonite. It was revealed that the most probable defect models are replacement of Al atoms sited in the five-coordinated M2 and six-coordinated M4 positions. Cell volume and lattice parameters of unit cells with different substitution defects of Al by Ti were optimized. The most stable structural models (the lowest free energy models) undergo more significant lattice deformations (biggest values of the *a*/*c* ratio) as a result of deformation. For the most probable structures of Ti-bearing hibonite the Ti *K* edge X-ray absorption near-edge structure spectra were simulated. A difference in XANES spectra of non-optimized and optimized structural models of substitution of M2 and M4 positions by Ti was shown. Energy shift of the features of XANES spectra calculated for optimized models towards the lower energies is in a good agreement (according to the Natoli's rule) with increase of Ti–O interatomic distances as a result of the structure optimization. The increase of the pre-edge feature of the Ti *K* edge XANES is observed when Ti coordination decreases. For more detailed analysis of local atomic structure and oxidation state of Ti atoms in investigated samples the comparison analysis of obtained theoretical Ti *K* edge XANES spectra with the experimental one is needed.

This study was supported by the grant of Russian Foundation for Basic Research (RFBR) 14-05-00580 "Nanodiagnostics of microelements environment in geological materials: X-ray investigation and computer modelling".

Authors are grateful to A. M. Walker (University of Leeds) and A. J. Berry (Australian National University) for collaboration on the project.

REFERENCES

1. Y. Amelin, A. N. Krot, A. A. Ulyanov, and I. D. Hutcheon, *Science*, **297**, 1678 (2002).
2. A. T. Anderson Jr., A. V. Crewe, J. R. Goldsmith, et al., *Science*, **167**, 587 (1970).
3. H. Curien, C. Guillemin, J. Orcel, and M. Sternberg, *C. R. Acad. Sci.,* Paris, 2845 (1956).
4. K. Kato and H. Saalfeld, *Neues Jahrb. Mineral., Abh*., **109**, 192 (1968).
5. A. A. Utsunomiya, K. Tanaka, H. Morikawa, et al., *J. Solid State Chem*., **75**, 197 (1988).
6. V. V. Bermanec, D. Holtstam, D. Sturman, et al., *Can. Mineral*., **34**, 1287 (1996).
7. A. M. Hofmeister, B. Wopenka, and A. J. Locock, *Geochim. Cosmochim. Acta*, **68**, 4485 (2004).
8. M. Nagashima, T. Armbruster, and T. Hainschwang, *Mineral. Mag*., **74**, 871 (2010).
9. R. G. Burns and V. M. Burns, *J. Geophys. Res*., **89**, 313 (1984).
10. J. R. Beckett, D. Live, F.-D. Tsay, et al., *Geochim. Cosmochim. Acta*, **52**, 1479 (1988).
11. P. M. Doyle, P. F. Schofield, A. J. Berry, et al., *Am. Mineral*., **99**, 1369 (2014).
12. G. Bunker, *Introduction to XAFS. A Practical Guide to X-ray Absorption Fine Structure Spectroscopy*, Cambridge University Press, UK (2010).
13. G. Kresse and J. Furthmüller, *Phys. Rev. B*, **54**, No. 16, 11169 (1996).
14. J. P. Perdew, K. Burke, and M. Ernzerhof, *Phys. Rev. Lett*., **77**, 3865 (1996).
15. D. M. Bylander, L. Kleinmann, and S. Lee, *Phys. Rev. B*, **42**, 1394 (1990).
16. E. L. Frank, W. J. Daniel, W. Boisvert, et al., *Conf. Proc*. (2010).
17. J. J. Rehr, J. J. Kas, F. D. Vila, et al., *Phys. Chem. Chem. Phys*., **12**, 5503 (2010).

18. J. J. Rehr, J. J. Kas, M. P. Prange, et al., *C. R. Phys*., **10**, No. 6, 548 (2009).
19. Y. Joly, *Phys. Rev. B*, **63**, 125120 (2001).
20. S. A. Guda, A. A. Guda, M. A. Soldatov, et al., *J. Chem. Theor. Comput*., **11**, No. 9, 4512-4521 (2015).
21. A. N. Kravtsova, S. A. Suchkova, M. B. Fayn, and A. V. Soldatov, *J. Struct. Chem*., **57**, No. 3, 491 (2016).
22. A. N. Kravtsova, K. A. Lomachenko, A. V. Soldatov, et al., *J. Electron Spectrosc. Relat. Phenom*., **195**, 189 (2014).
23. I. S. Rodina, A. N. Kravtsova, A. V. Soldatov, and A. J. Berry, *Opt. Spectrosc*., **111**, No. 6, 936 (2011).
24. I. S. Rodina, A. N. Kravtsova, A. V. Soldatov, et al., *Opt. Spectrosc*., **115**, No. 6, 858 (2013).
25. A. Bianconi, M. Dell Ariccia, A. Gargano, and C. R. Natoli, in: *Bond Length Determination Using XANES, EXAFS and Near Edge Structure*, A. Bianconi, A. Incoccia, and S. Stipcich (eds.), Springer, Berlin (1987), p. 57.